Green Synthesis of Zinc Oxide Nanoparticles (ZnO NPs) and Adsorption with Cibacron Brillant Yellow (CBY) dye

Alieaa Hafudh Obaid[1], Fadhila M. Hussein[1], SalmaAbd al-Rudha Abbas[1], and Tahseen ali Ibrahim[2]

[1]Department of Chemistry, College of Science, University of Al-Mustansiriyah, Baghdad, Iraq.

[2]Ministry of Health, Inspection Department, Baghdad, Iraq.

Abstract

In this work, zinc oxide (ZnO) nanoparticles are synthesized by the green synthesis. scanning electron microscopy measurements, X-ray diffraction technique to determine their crystal structure, and FTIR are used to analyze the ZnO nanoparticles. The green synthesis ZnO nanoparticles perform as a good adsorbent for the Cibacron Brillant Yellow (CBY) dye in aqueous solutions. The effects of adsorbent mass, contact time, temperature, and dye concentration of Cibacron Brillant Yellow (CBY) were investigated. The dye isotherm adsorption of Cibacron Brillant Yellow (CBY) exhibited an excellent Compatibility with Freundlich isotherm models The ΔS, ΔH, and ΔG parameters were calculated using a thermodynamic research, yielding 0.01486493 kJ/mol, 63.955422 J/mol K, and -19.3636279 kJ/mol, respectively. The kinetic analysis also revealed that the adsorption was pseudo-first-order.

Keywords: zinc oxide (ZnO) nanoparticl; Adsorption; Cibacron Brillant Yellow (CBY) dye ; green synthesis

1.Introduction.

Zinc oxide nanoparticles (ZnO NPs), are among the very important metal oxide nanoparticles, Because of the physical and chemical properties of zinc oxide, it is used in many fields [1]. ZnO NPs was used for the first time in the rubber industry to supply wear resistance to rubber compounds and to improve durability, intensity, antiaging, and other functions of high polymers [2]. ZnO is widely used in personal care products, such as sunscreen and cosmetics, due to its strong UV absorption capabilities [3].Moreover, ZnO NPs have good antimicrobial and antibacterial, in textile sector, fabrics completed with ZnO NPs have shown the catchy functions of UV, antibacterial, deodorant , Also visible light resistant [4]. In addition to the aforementioned applications, zinc oxide can be utilized in a variety of different industries, such as concrete manufacture, photocatalysis, electronics, and electro technology [5].Zinc is widely recognized as an essential trace element , it is present in all tissues of the body, including the muscle, brain, skin, and bone. Zinc is important component of many enzyme systems and plays an essential role in protein and nucleic acid production, hematopoiesis, and neurogenesis [2].ZnO NPs is often used as a food additive because of its small particle size, which allows zinc to be absorb more quickly for the body . zinc oxide (ZnO) is also designated as a "GRAS" (generally recognized as safe) compound by the US Food and Drug Administration (FDA)[6]. ZnO NPs have gotten a lot of attention in

biomedical applications because of these features. ZnO NPs which are less toxic and less expensive than other metal oxide nanoparticles , have a wide range of medical applications., including anticancer, drug delivery, antibacterial, and diabetic treatment; anti-inflammation; wound healing; and bio imaging[7].

Adsorption At the boundary between two phases, several physical, chemical, and biological activities occur. Adsorption is the change in concentration of a specific substance at the interface as compared to nearby phases., the types of phases that link, could be in the following systems: Solid-liquid, solid-gas, liquid-liquid, and liquid-gas [8]The adsorbent is the material to which the adsorbate is attached, while the adsorbate is the substance that is attached to the surface[9].One of the most extensively used techniques for pollutant removal from polluted media is adsorption. Activated carbon, molecular screens, polymeric adsorbents, and other low-cost materials are some of the most used adsorbents [10].Adsorption is not the same as absorption, which occurs when a substance diffuses into a solid or liquid to form a solution. Absorption is a bulk phenomena, whereas adsorption is a surface juvenile [11]. To our knowledge, no methodical data on the adsorption ways of Cibacron Brillant Yellow (CBY) dye using ZnO nanoparticles has been studied. Cibacron Brillant Yellow (CBY) dye was separated from its aqueous solutions using ZnO nanoparticles synthesized using the green synthsis method. In this study, the mass of adsorbent, the period of surface contact, temperature, and CBY dye concentration were all taken into account.

2.1. Materials

Powder Zinc Nitrate Hexahydrate (Zn $(NO_3)_2.6H_2O$), Plant Orange Peel extract ,NaOH, Sigma-Aldrich products were purchased and used exactly as they were given to us (UK). Throughout the purification of the finished product, deionized water was employed.

2.2. Preparation ZnO NPs.

Plant Orange Peel extract was added drop wise with stirring at room temperature to a solution of zinc nitrate hexahydrate ($Zn(NO_3)_2.6H_2O$) (0.1M , 400 ml)for (1.5)hrs until The solution is cloudy (evidence of nanoparticle formation) then was added a (0.05)M of NaOH, then the precipitate was washed numerous times with deionized water for two days before being dried at 120 °C in the oven for two hours, then calcination at (450)°C for three hours ,Adding the base to the nitrate solution contributes to the formation of zinc hydroxide in the aqueous medium. Also see it in the following equations [12]

$$Zn(NO_3)_2.6H_2O + 2NaOH \rightarrow Zn(OH)_2 + 2NaNO_3 + 6H_2O \text{ -------(1)}$$

$$Zn(OH)_2 + 2H_2O \rightarrow Zn^{+} + 2OH^{-} + 2H_2O \rightarrow Zn(OH)^{-2}_4 + 2H \text{ ------(2)}$$

$$Zn(OH)^{-2}_4 \xrightarrow{(450)°C\ ,3hr} ZnO + H_2O + 2OH^{--} \text{ ------(3)}$$

2.3. Characterization.

The ZnO nanoparticles were analyzed using X-ray diffraction (XRD-6000), which was operated at 40 kV and 30 mA to produce 1.5406 °A wavelength radiation. JEM-2100 JEOL

(Japan), AFM photos of (ZnO) nanoparticles and their size distributions, AFM is used for morphological study because it creates topological images of surfaces at a very high magnification and makes it easier to see the atomic structure of crystals. The diameters of ZnO nanoparticles were determined using scanning electron microscopy (SEM). The spectrum of ZnO nanoparticle was demonstrated using Fourier-transform infrared spectrophotometer(FTIR) Shimadzu 4800S (USA).

2.4.Adsorption of Cibacron Brillant Yellow (CBY)dye on ZnO

(500 ml) solution was prepared from the stock solution (30 ppm) of Cibacron Brillant Yellow (CBY) dye at different concentrations between (5-25ppm) by dissolving (CBY) dye deionized water. ZnO nanoparticles (0.008gm) were added to various solutions and shackled for 60 minutes at different temperatures: 15°C, 30°C, 45°C, and 60°C. These solutions were filtered and put through a UV-VIS spectrophotometer to determine the concentration of CBY dye in the filtrate, using the equation below [13] [14].

$Qe= (C_0-Ce)\ Vsol\ /M$ ------(4)

where Qe (mg/g) is the equilibrium adsorption capacity, C0 and Ce are the initial and equilibrium CBY dye concentrations (mg/L), Vsol is the liquid volume (L), and M is the weight of the ZnO nanoparticle (g) .

3.Results and discussion.

3.1. Characterization of ZnO nanoparticale .

To determine the nature of the powders produced, all samples were subjected to XRD analysis.. Figure 1 depicts the XRD peaks of the ZnO crystal-style structure at angles ranging from 20° to 80°. According to the standard ZnO nanoparticle patterns, the high peaks at 31.82°, 34.79°,36.43°,47.73°,56.36°,63.25°,68,41°,and 77,18° which are corresponding to 100,002,101,102,110,103,112,and004 Müller values, respectively as shown in Figure(1). FTIR spectral analysis of ZnO nanoparticle is shown in figure(2). The bond at 545 cm^{-1} and 410 cm^{-1} belongs to the ZnO bonds (bending vibration) due to the bending vibration of Zn-O, this agrees with the results of Z. N. Kayani G et al[15] who reported that the broad band at 400-700 cm^{-1} refers to Zn-O bending vibrations [15]Other researchers confirmed that the peaks at 667.3cm^{-1} observed in the FTIR spectrum are due to Zn-O vibration [16] The bands at 1585.19 due to vibration of υ(C=C) [17] The peak at 3515cm^{-1}, represents the stretching vibration of the O-H group[16] The peak at 1474.46 cm^{-1} and 1354.84 cm^{-1} indicating the C-H bending of alkanes[18] as shown in Figure(2). SEM was used to evaluate the shape and size of the primary nanopaticle, as shown in Figure(3).

3.2 Adsorption Isotherm.

The most essential part of the adsorption investigation was determining how adsorbent CBY dye is by fitting isotherm adsorption results with adsorption results. This study took into account Freundlich and Langmuir's isotherms. As shown in (Fig. 4), the R^2 correlation factor shows that Freundlich isotherm equations suit the adsorption results fairly well ,demonstrated

in figure (4 a). The following equation is the linearized form of Freundlich adsorption[19][20].

$\log Q_e = \log K_{Fr} + (1/nf) \log C_e$---------- (5)

where the indices of adsorption capacity and intensity, kf and n, are also known as the Freundlich constants. The intercept is used to determine the kf, while the slope is used to calculate the n. The Freundlich isotherm for ZnO was computed 1/n, which was 0.541, in this study. This conclusion was consistent with physical adsorption being beneficial. The data, however, did not fit the Langmuir adsorption isotherm, as indicated in the equation below [21] [22].

$Ce / qe = 1 / q_{max} K_L + Ce / q_{max}$ -------(6)

Where qe is the amount of dye adsorbed at equilibrium (mg/g), Ce is the adsorbate concentration at equilibrium (mg/L), KL is the Langmuir isotherm constant (L/mg), and qmax is the maximal monolayer coverage capacity (mg/g). The rate of adsorption was relent less from the linear equation of specific adsorption Ce⁄Qe vs Ce. demonstrated in figure (4 b).

$R_L = 1/ (1 + K_L C_i)$ ---------- (7)

where Ci: represents is the initial concentration of CBY dye(mg/L), The RL values are all between 0 and 1, showing that CBY dye adsorption on ZnO nanoparticles is preferred.

3.3 The influence of contact time.

was examined at 10 mg/L concentration of CBY dye with 0.008g ZnO nanoparticle from(10-90)min at 303K and shaking speed (3000 rpm).However, it can be seen from Figure (5) that The amount of adsorption increases directly with the increase in the concentration of the dye which the adsorption of CBY occurred quickly from the beginning then reached a steady state at 60 minutes. This could be because the nanoparticles' surfaces have a lot of empty adsorption sites., which then increase until the time reaches 60 to reach equilibrium [23]

3.4 The influence of Dye Concentrations

The influence of the concentration (CBY)dye on ZnO nanoparticles was experimentally studied under the following conditions: the dye concentration range is (5, 10, 15, 20 and 25) mg/L, and the mass of nanoparticles is (0.006) g, volume 15 ml, at 303K, the stirring time is 60 minutes,. It can be seen from Figure (6) that when the dye concentration increases from 5 to 25 mg/L, It can be proposed that an increase in the CBY concentration leads to an increase adsorption. We suggest, increase in adsorption because of the increase in the number of effective sites with increase the concentration[23]

3.5 The weight effect of ZnO nanoparticles.

The effect quantity of the adsorbent material on the dye adsorption rate by ZnO nanoparticles as an adsorbent was performed using various nanoparticles weight (0.004, 0.006, 0.008,0.01 and 0.012 g) and 15 ml of 10 mg/L dye ,303 K, the stirring time is 60 minutes, We have

noticed The amount of CBY dye adsorption solution increased as the weight of ZnO NPs increased. Because of the increased active site of ZnO nanoparticles, the adsorption rate is rapid, as shown in Figure (7). And , increased adsorption of dye was shown by increasing the amount of adsorbent [23]

3.6. Temperature effect and calculation of thermodynamic parameters.

At temperatures of 288, 303, 318, and 333 k, the temperature effect of Cibacron Brillant Yellow (CBY) dye adsorption on the ZnO nanoparticles' surface was investigated. The amount of dye adsorption solution increased when the temperature was raised, as seen in fig (8). This indicates that the process was endothermic, with a positive ΔH mean. Both absorption and adsorption processes were demonstrated in this way[4]. The thermodynamic parameters supply a lot of information about the intrinsic energy changes that occur during adsorption. Using the adsorption free energy (ΔG), enthalpy (ΔH), and entropy (ΔS) The following changes were calculated using following equations to forecast the adsorption process.[19] [19][24][25][26] [27]

$$\mathbf{Ln K_{eq} = -\Delta H/RT + \Delta S/R} \quad \text{(8)}$$

$$\mathbf{K_{eq} = q_e/C_e} \quad \text{(9)}$$

$$\mathbf{\Delta G = \Delta H - T\Delta S} \quad \text{(10)}$$

Where: T: is the absolute temperature (K), Keq: is the ability of adsorbate to retain and a measure of its movement within the solution, R: is the general of gases constant(8.31 j. K^{-1} $mole^{-1}$), *qe* (mg/gm) is the equilibrium capacity of adsorption, The slop and intercept of the linear Vants Hoff plot of lnKeq vs 1/T can be used to determine the values of ΔH and ΔS, respectively demonstrated in Figure (9).The slope's corresponding ΔH was (0.01486493 kJ/mol), Indicates that the process was endothermic. The ΔS value from the intercept was (63.955422 J/(mol.K)), showing that the adsorbed molecules were still moving on the surface due to both absorption and adsorption. The adsorption of CBY dye was aided by a higher temperature. The adsorption ΔG was calculated to be(- 19.3636279 kJ/mol), indicating that adsorption occurred spontaneously.

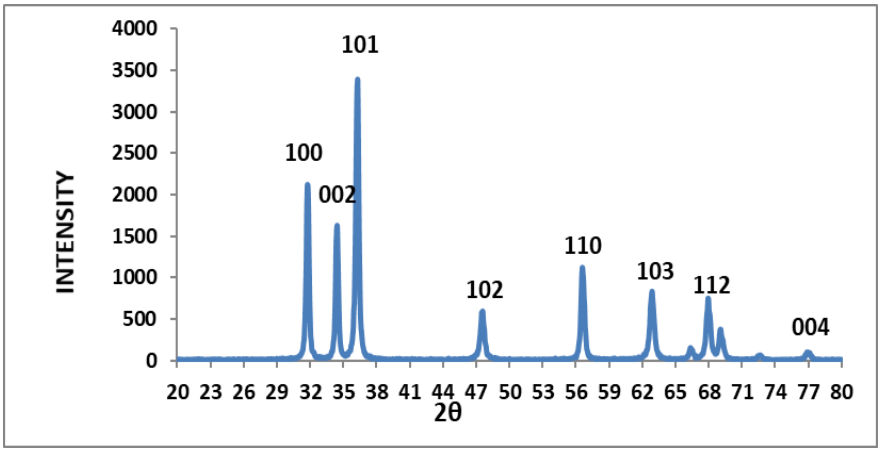

Fig. (1) X-ray diffraction XRD for ZnO NPs.

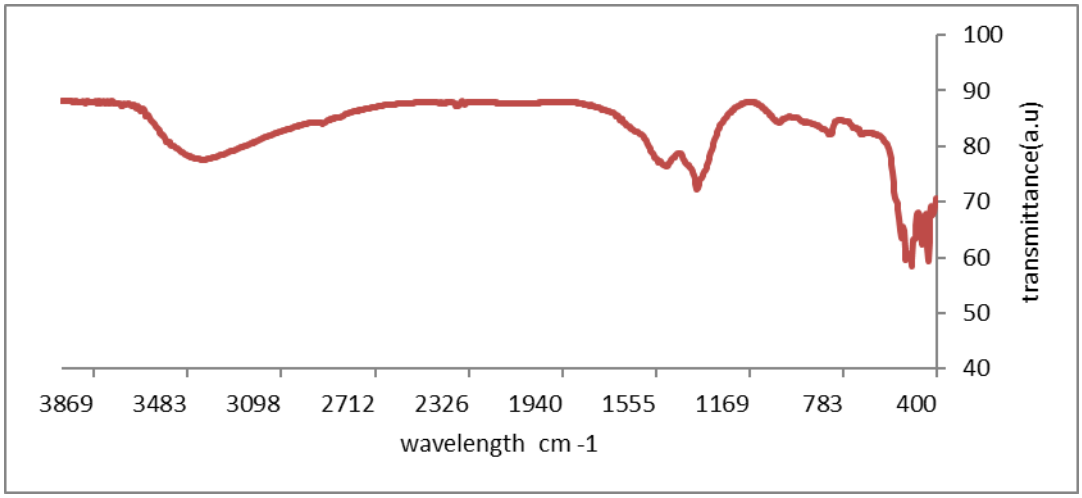

Fig. (2) FTIR spectra of ZnO.

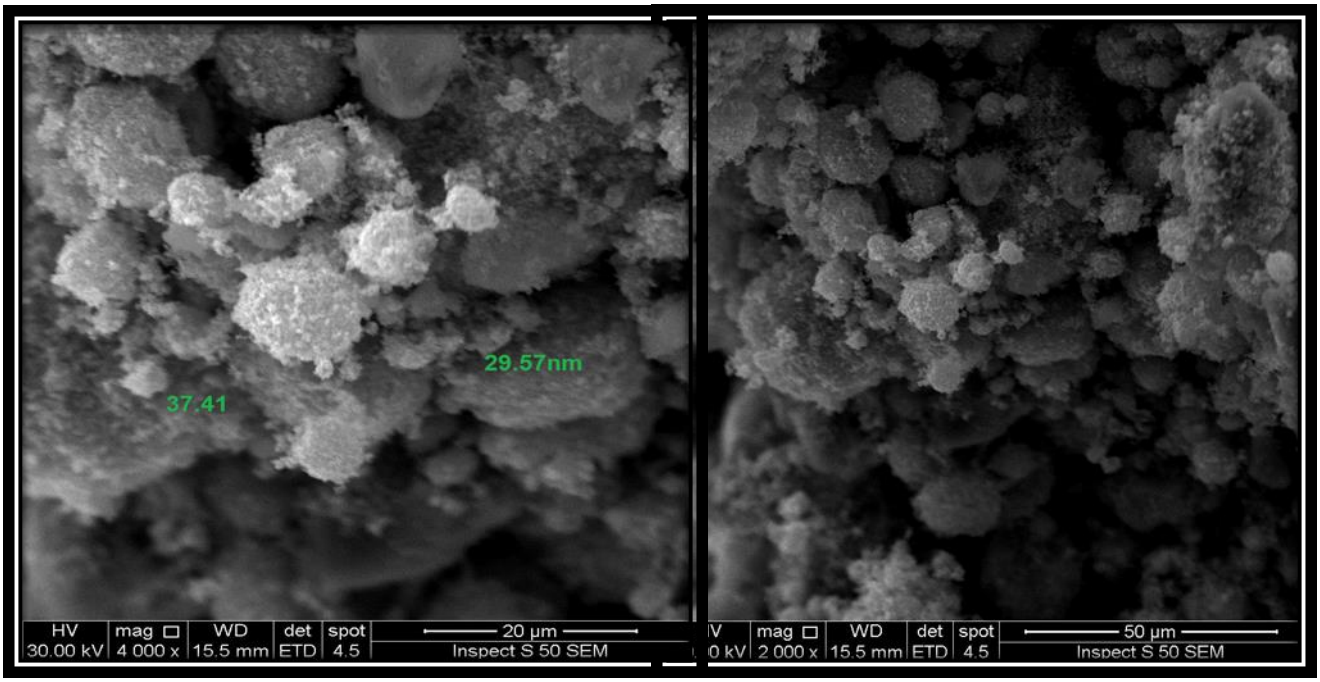

Fig. 3. SEM micrographs of the ZnO nanoparticles.

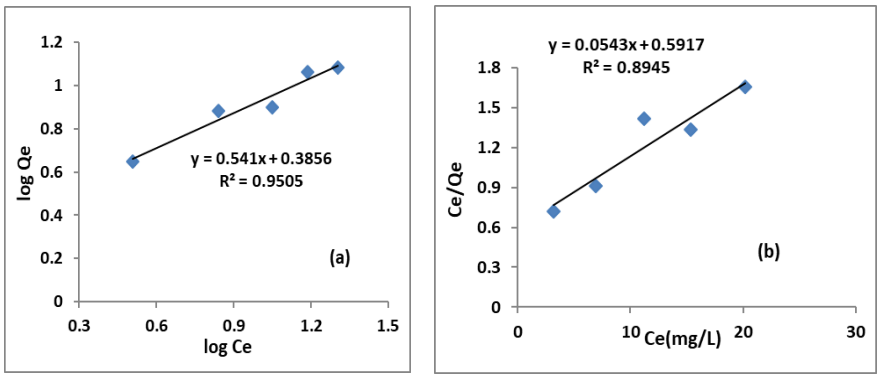

Fig.4. Adsorption curve of (a) Freundlich isotherm ,(b) Langmuir isotherm at 303 K

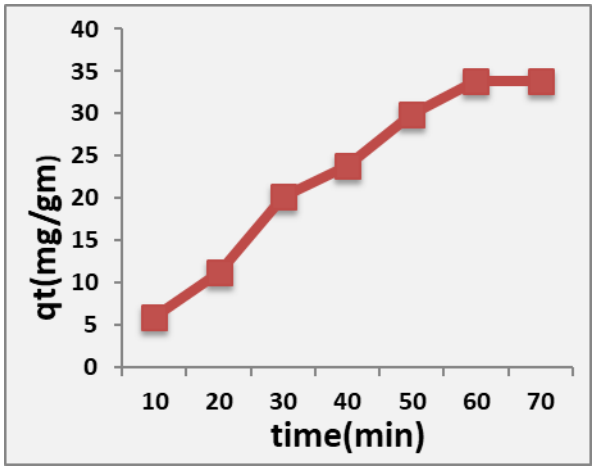

Fig. (5): The influence of contact time

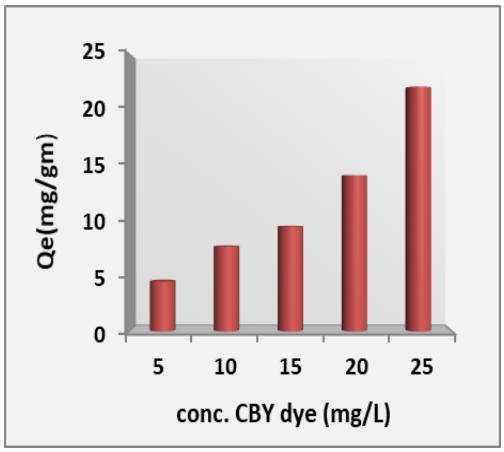

Fig. (6) Effect of Concentration CBY dye

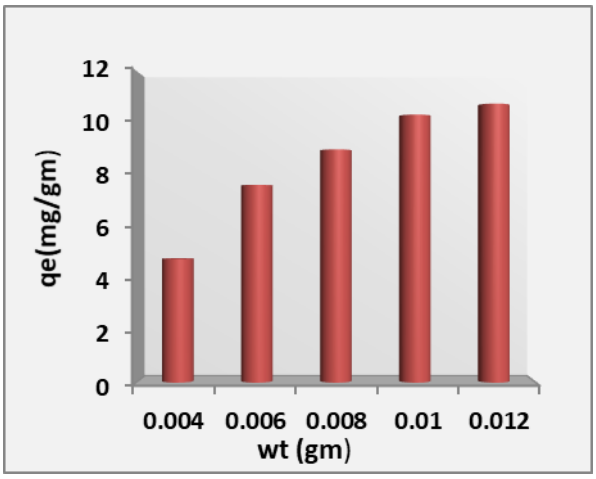

Fig. (7):The weight effect of ZnO NPs

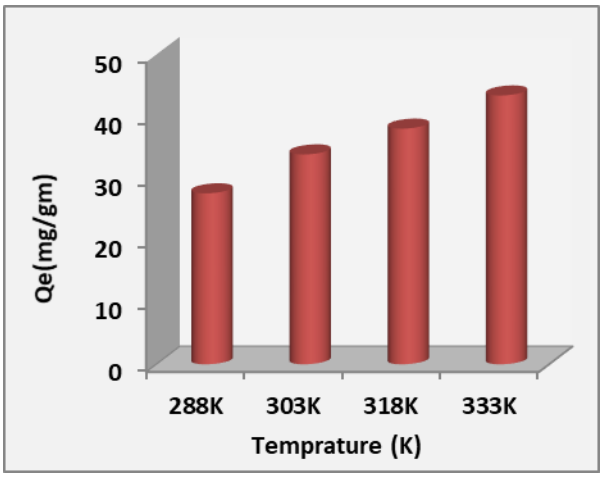

Fig.(8):Temperatureinfluenceonthe adsorption

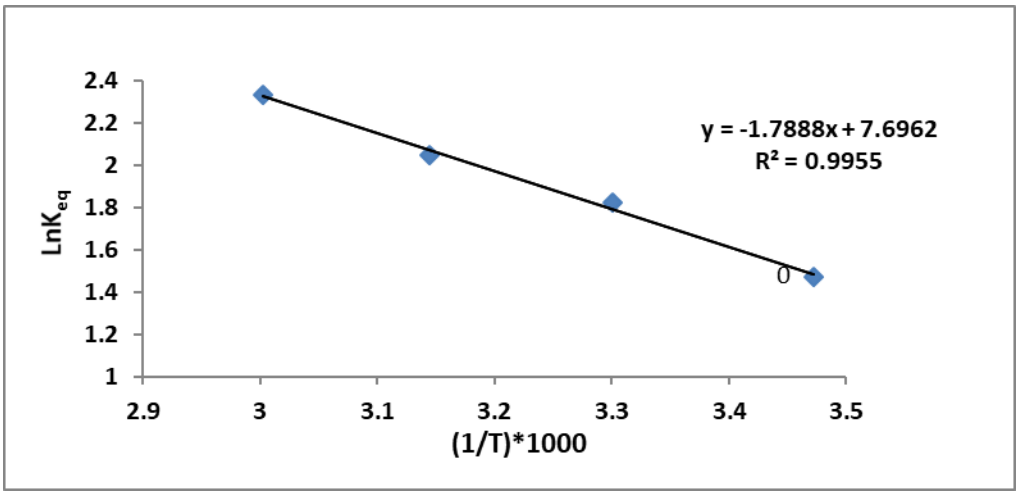

Figure (9): Van't Hoff plots of the dye adsorption at different temperatures.

3.7. 3.7 Dynamics.

The surface adsorption dynamics of CBY dye ZnO nanoparticle adsorbents are critical in adsorbent applications. The adsorption equilibrium time for 0.008 g of ZnO NPs adsorbents was found to be around 60 minutes in the study of CBY dye. Furthermore, in this study, The following classical and kinetic models were employed to depict the above-mentioned adsorption data: A pseudo-first-order model emerges from the equation. (11)[21] [28][29]

$$\ln (q_e - q_t) = \ln q_e - k_1 .t \text{ ---------- (11)}$$

Pseudo-second order kinetic model is given by the equation (12) [19][30].

$$t / qt = 1 / k_2 qe^2 + (1/qe).t \text{ ---------- (12)}$$

where , qe, and qt denote the number of adsorbent CBY dye (mg/g) at equilibrium and time, respectively, and k1 and k2 denote the kinetic rate constants. Furthermore,Depending on the graph of the figure (10), it is clear that it depends on the false first order pseudo first- order kinetic models.

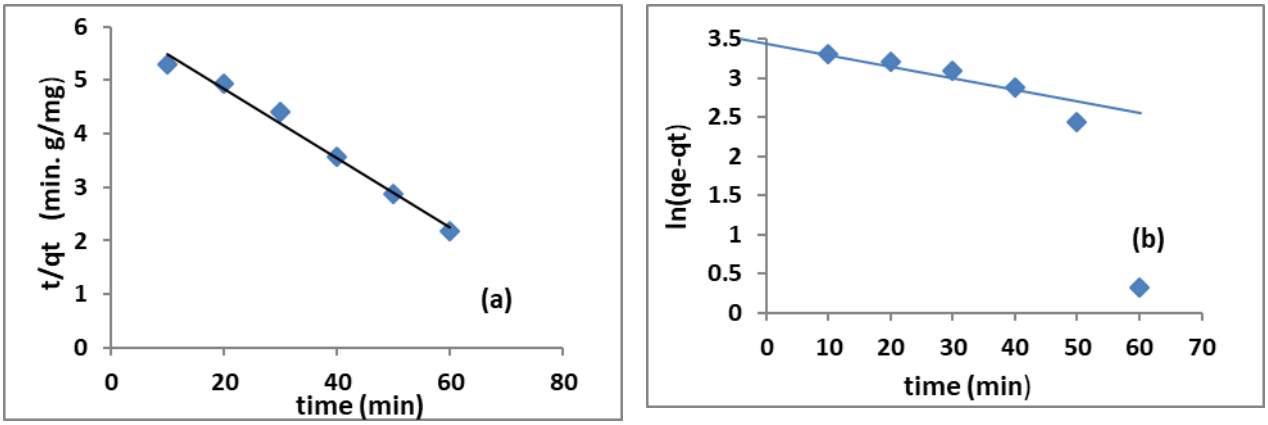

Fig.10. Dynamic adsorption of CBY dye : (a)pseudo-first-order and (b)pseudo-second-order.

4. Conclusion

The green synthesis method produced high-quality ZnO NPs, as determined by XRD, SEM, and FTIR characterizations. The results of all of the characterisation methods were identical. proving that the synthesized ZnO was nanoparticl, with an average crystal size of 70.75 nm. The nanoparticl demonstrated excellent adsorption properties in the removal of CBY dye from aqueous solutions. The efficiency of ZnO nanoparticl adsorption was demonstrated in both kinetic and dynamic studies. The results were well fitted by Freundlich isotherm models. The thermodynamic parameters were calculated, and the adsorption values for ΔH, ΔS, and ΔG were 0.01486493 kJ/mol, 63.955422 J/mol K, and -19.3636279 kJ/mol, repectively. These findings demonstrate that Adsorption is a spontaneous endothermic process.. It is clear from the graph in figure ten that it is dependent on the false first order pseudo first-order kinetic models.

Refrence

[1] J. A. Ruszkiewicz, A. Pinkas, B. Ferrer, T. V Peres, A. Tsatsakis, and M. Aschner, “Neurotoxic effect of

active ingredients in sunscreen products, a contemporary review," *Toxicol. reports*, vol. 4, pp. 245–259, 2017.

[2] A. Kołodziejczak-Radzimska and T. Jesionowski, "Zinc oxide—from synthesis to application: a review," *Materials (Basel).*, vol. 7, no. 4, pp. 2833–2881, 2014.

[3] M. D. Newman, M. Stotland, and J. I. Ellis, "The safety of nanosized particles in titanium dioxide–and zinc oxide–based sunscreens," *J. Am. Acad. Dermatol.*, vol. 61, no. 4, pp. 685–692, 2009.

[4] A. Hatamie *et al.*, "Zinc oxide nanostructure-modified textile and its application to biosensing, photocatalysis, and as antibacterial material," *Langmuir*, vol. 31, no. 39, pp. 10913–10921, 2015.

[5] F.-X. Xiao, S.-F. Hung, H. B. Tao, J. Miao, H. Bin Yang, and B. Liu, "Spatially branched hierarchical ZnO nanorod-TiO 2 nanotube array heterostructures for versatile photocatalytic and photoelectrocatalytic applications: towards intimate integration of 1D–1D hybrid nanostructures," *Nanoscale*, vol. 6, no. 24, pp. 14950–14961, 2014.

[6] J. W. Rasmussen, E. Martinez, P. Louka, and D. G. Wingett, "Zinc oxide nanoparticles for selective destruction of tumor cells and potential for drug delivery applications," *Expert Opin. Drug Deliv.*, vol. 7, no. 9, pp. 1063–1077, 2010.

[7] H. Xiong, "ZnO nanoparticles applied to bioimaging and drug delivery," *Adv. Mater.*, vol. 25, no. 37, pp. 5329–5335, 2013.

[8] S. P. Suriyaraj, T. Vijayaraghavan, P. Biji, and R. Selvakumar, "Adsorption of fluoride from aqueous solution using different phases of microbially synthesized TiO2 nanoparticles," *J. Environ. Chem. Eng.*, vol. 2, no. 1, pp. 444–454, 2014.

[9] R. B. Anderson, *Experimental Methods in Catalytic Research: Physical Chemistry: A Series of Monographs*, vol. 1. Academic Press, 2013.

[10] S. Malamis and E. Katsou, "A review on zinc and nickel adsorption on natural and modified zeolite, bentonite and vermiculite: examination of process parameters, kinetics and isotherms," *J. Hazard. Mater.*, vol. 252, pp. 428–461, 2013.

[11] G. A. Somorjai and Y. Li, *Introduction to surface chemistry and catalysis*. John Wiley & Sons, 2010.

[12] P. K. Samanta, S. K. Patra, A. Ghosh, and P. R. Chaudhuri, "Visible emission from ZnO nanorods synthesized by a simple wet chemical method," *Int. J. Nanosci. Nanotechnol*, vol. 1, no. 1–2, pp. 81–90, 2009.

[13] L. Svecova *et al.*, "Sorption of selenium oxyanions on TiO2 (rutile) studied by batch or column experiments and spectroscopic methods," *J. Hazard. Mater.*, vol. 189, no. 3, pp. 764–772, 2011.

[14] M. A. Mohammed, A. M. Rheima, S. H. Jaber, and S. A. Hameed, "The removal of zinc ions from their aqueous solutions by Cr2O3 nanoparticles synthesized via the UV-irradiation method," *Egypt. J. Chem.*, vol. 63, no. 2, pp. 425–431, 2020.

[15] Z. N. Kayani, I. Shah, B. Zulfiqar, S. Riaz, S. Naseem, and A. Sabah, "Structural, optical and magnetic properties of nanocrystalline Co-Doped ZnO thin films grown by Sol–Gel," *Zeitschrift für Naturforsch. A*, vol. 73, no. 1, pp. 13–21, 2018.

[16] N. Tummapudi, S. Modem, N. K. Jaladi, G. Choudary, and S. R. Kurapati, "Structural, morphological, optical and mechanical studies of annealed ZnO nano particles," *Phys. B Condens. Matter*, vol. 597, p. 412401, 2020.

[17] A. M. Awwad, M. W. Amer, N. M. Salem, and A. O. Abdeen, "Green synthesis of zinc oxide nanoparticles (ZnO-NPs) using Ailanthus altissima fruit extracts and antibacterial activity," *Chem. Int*, vol. 6, no. 3, pp. 151–159, 2020.

[18] P. Verma and S. K. Samanta, "Continuous ultrasonic stimulation based direct green synthesis of pure anatase-TiO2 nanoparticles with better separability and reusability for photocatalytic water decontamination," *Mater. Res. Express*, vol. 5, no. 6, p. 65049, 2018.

[19] D. H. Hussain, A. M. Rheima, and S. H. Jaber, "Cadmium ions pollution treatments in aqueous solution using electrochemically synthesized gamma aluminum oxide nanoparticles with DFT study," *Egypt. J. Chem.*, vol. 63, no. 2, pp. 417–424, 2020.

[20] A. M. Rheima, D. H. Hussain, and M. M. A. Almijbilee, "Graphene-silver nanocomposite: Synthesis, and adsorption study of cibacron blue dye from their aqueous solution," *J. Southwest Jiaotong Univ.*, vol. 54, no. 6, 2019.

[21] A. M. Rheima, M. A. Mohammed, S. H. Jaber, and S. A. Hameed, "Adsorption of selenium (Se4+) ions pollution by pure rutile titanium dioxide nanosheets electrochemically synthesized," *Desalin. Water Treat.*, vol. 194, no. 2020, pp. 187–193, 2020.

[22] N. Ammar, A. Fahmy, S. Kanawy Ibrahim, E. M. A. Hamzawy, and M. El-Khateeb, "Wollastonite ceramic/CuO nano-Composite For cadmium ions removal from waste water," *Egypt. J. Chem.*, vol. 60, no. 5, pp. 817–823, 2017.

[23] R. Ghibate, O. Senhaji, and R. Taouil, "Kinetic and thermodynamic approaches on Rhodamine B adsorption onto pomegranate peel," *Case Stud. Chem. Environ. Eng.*, vol. 3, p. 100078, 2021.

[24] A. Safri, A. J. Fletcher, E. Abdel-Halim, M. A. Ismail, and A. Hashem, "Calligonum crinitum as a novel sorbent for sorption of Pb (II) from aqueous solutions: thermodynamics, kinetics, and isotherms," *J. Polym. Environ.*, vol. 29, no. 5, pp. 1505–1515, 2021.

[25] E. C. Lima, A. A. Gomes, and H. N. Tran, "Comparison of the nonlinear and linear forms of the van't Hoff equation for calculation of adsorption thermodynamic parameters (Δ S° andΔ H°)," *J. Mol. Liq.*, vol. 311, p. 113315, 2020.

[26] W. Wu, C. Lu, M. Yuan, Y. Tian, and H. Zhou, "Acidification of potassium bismuthate for enhanced visible-light photocatalytic degradation ability: an effective strategy for regulating the abilities of adsorption, oxidation, and photocatalysis," *Appl. Surf. Sci.*, vol. 544, p. 148873, 2021.

[27] M. Zulfiqar *et al.*, "Effect of organic solvents on the growth of TiO2 nanotubes: An insight into photocatalytic degradation and adsorption studies," *J. Water Process Eng.*, vol. 37, p. 101491, 2020.

[28] A. A. A. Darwish, M. Rashad, and H. A. AL-Aoh, "Methyl orange adsorption comparison on nanoparticles: Isotherm, kinetics, and thermodynamic studies," *Dye. Pigment.*, vol. 160, pp. 563–571, 2019.

[29] F. Wang, "Adsorption of Anionic Dye on Graphene Nanosheets Doped with Ag Nanoparticles: Kinetics and Thermodynamic Study," *Russ. J. Phys. Chem. A*, vol. 93, no. 7, pp. 1357–1364, 2019.

[30] A. E. Regazzoni, "Adsorption kinetics at solid/aqueous solution interfaces: on the boundaries of the pseudo-second order rate equation," *Colloids Surfaces A Physicochem. Eng. Asp.*, vol. 585, p. 124093, 2020.

[1] J. A. Ruszkiewicz, A. Pinkas, B. Ferrer, T. V Peres, A. Tsatsakis, and M. Aschner, "Neurotoxic effect of active ingredients in sunscreen products, a contemporary review," *Toxicol. reports*, vol. 4, pp. 245–259, 2017.

[2] A. Kołodziejczak-Radzimska and T. Jesionowski, "Zinc oxide—from synthesis to application: a review," *Materials (Basel).*, vol. 7, no. 4, pp. 2833–2881, 2014.

[3] M. D. Newman, M. Stotland, and J. I. Ellis, "The safety of nanosized particles in titanium dioxide–and zinc oxide–based sunscreens," *J. Am. Acad. Dermatol.*, vol. 61, no. 4, pp. 685–692, 2009.

[4] A. Hatamie *et al.*, "Zinc oxide nanostructure-modified textile and its application to biosensing, photocatalysis, and as antibacterial material," *Langmuir*, vol. 31, no. 39, pp. 10913–10921, 2015.

[5] F.-X. Xiao, S.-F. Hung, H. B. Tao, J. Miao, H. Bin Yang, and B. Liu, "Spatially branched hierarchical ZnO nanorod-TiO 2 nanotube array heterostructures for versatile photocatalytic and photoelectrocatalytic applications: towards intimate integration of 1D–1D hybrid nanostructures," *Nanoscale*, vol. 6, no. 24, pp. 14950–14961, 2014.

[6] J. W. Rasmussen, E. Martinez, P. Louka, and D. G. Wingett, "Zinc oxide nanoparticles for selective destruction of tumor cells and potential for drug delivery applications," *Expert Opin. Drug Deliv.*, vol. 7, no. 9, pp. 1063–1077, 2010.

[7] H. Xiong, "ZnO nanoparticles applied to bioimaging and drug delivery," *Adv. Mater.*, vol. 25, no. 37, pp. 5329–5335, 2013.

[8] S. P. Suriyaraj, T. Vijayaraghavan, P. Biji, and R. Selvakumar, "Adsorption of fluoride from aqueous solution using different phases of microbially synthesized TiO2 nanoparticles," *J. Environ. Chem. Eng.*, vol. 2, no. 1, pp. 444–454, 2014.

[9] R. B. Anderson, *Experimental Methods in Catalytic Research: Physical Chemistry: A Series of Monographs*, vol. 1. Academic Press, 2013.

[10] S. Malamis and E. Katsou, "A review on zinc and nickel adsorption on natural and modified zeolite, bentonite and vermiculite: examination of process parameters, kinetics and isotherms," *J. Hazard. Mater.*, vol. 252, pp. 428–461, 2013.

[11] G. A. Somorjai and Y. Li, *Introduction to surface chemistry and catalysis*. John Wiley & Sons, 2010.

[12] P. K. Samanta, S. K. Patra, A. Ghosh, and P. R. Chaudhuri, "Visible emission from ZnO nanorods synthesized by a simple wet chemical method," *Int. J. Nanosci. Nanotechnol*, vol. 1, no. 1–2, pp. 81–90,

2009.
[13] L. Svecova *et al.*, "Sorption of selenium oxyanions on TiO2 (rutile) studied by batch or column experiments and spectroscopic methods," *J. Hazard. Mater.*, vol. 189, no. 3, pp. 764–772, 2011.
[14] M. A. Mohammed, A. M. Rheima, S. H. Jaber, and S. A. Hameed, "The removal of zinc ions from their aqueous solutions by Cr2O3 nanoparticles synthesized via the UV-irradiation method," *Egypt. J. Chem.*, vol. 63, no. 2, pp. 425–431, 2020.
[15] Z. N. Kayani, I. Shah, B. Zulfiqar, S. Riaz, S. Naseem, and A. Sabah, "Structural, optical and magnetic properties of nanocrystalline Co-Doped ZnO thin films grown by Sol–Gel," *Zeitschrift für Naturforsch. A*, vol. 73, no. 1, pp. 13–21, 2018.
[16] N. Tummapudi, S. Modem, N. K. Jaladi, G. Choudary, and S. R. Kurapati, "Structural, morphological, optical and mechanical studies of annealed ZnO nano particles," *Phys. B Condens. Matter*, vol. 597, p. 412401, 2020.
[17] A. M. Awwad, M. W. Amer, N. M. Salem, and A. O. Abdeen, "Green synthesis of zinc oxide nanoparticles (ZnO-NPs) using Ailanthus altissima fruit extracts and antibacterial activity," *Chem. Int*, vol. 6, no. 3, pp. 151–159, 2020.
[18] P. Verma and S. K. Samanta, "Continuous ultrasonic stimulation based direct green synthesis of pure anatase-TiO2 nanoparticles with better separability and reusability for photocatalytic water decontamination," *Mater. Res. Express*, vol. 5, no. 6, p. 65049, 2018.
[19] D. H. Hussain, A. M. Rheima, and S. H. Jaber, "Cadmium ions pollution treatments in aqueous solution using electrochemically synthesized gamma aluminum oxide nanoparticles with DFT study," *Egypt. J. Chem.*, vol. 63, no. 2, pp. 417–424, 2020.
[20] A. M. Rheima, D. H. Hussain, and M. M. A. Almijbilee, "Graphene-silver nanocomposite: Synthesis, and adsorption study of cibacron blue dye from their aqueous solution," *J. Southwest Jiaotong Univ.*, vol. 54, no. 6, 2019.
[21] A. M. Rheima, M. A. Mohammed, S. H. Jaber, and S. A. Hameed, "Adsorption of selenium (Se4+) ions pollution by pure rutile titanium dioxide nanosheets electrochemically synthesized," *Desalin. Water Treat.*, vol. 194, no. 2020, pp. 187–193, 2020.
[22] N. Ammar, A. Fahmy, S. Kanawy Ibrahim, E. M. A. Hamzawy, and M. El-Khateeb, "Wollastonite ceramic/CuO nano-Composite For cadmium ions removal from waste water," *Egypt. J. Chem.*, vol. 60, no. 5, pp. 817–823, 2017.
[23] R. Ghibate, O. Senhaji, and R. Taouil, "Kinetic and thermodynamic approaches on Rhodamine B adsorption onto pomegranate peel," *Case Stud. Chem. Environ. Eng.*, vol. 3, p. 100078, 2021.
[24] A. Safri, A. J. Fletcher, E. Abdel-Halim, M. A. Ismail, and A. Hashem, "Calligonum crinitum as a novel sorbent for sorption of Pb (II) from aqueous solutions: thermodynamics, kinetics, and isotherms," *J. Polym. Environ.*, vol. 29, no. 5, pp. 1505–1515, 2021.
[25] E. C. Lima, A. A. Gomes, and H. N. Tran, "Comparison of the nonlinear and linear forms of the van't Hoff equation for calculation of adsorption thermodynamic parameters (Δ S° andΔ H°)," *J. Mol. Liq.*, vol. 311, p. 113315, 2020.
[26] W. Wu, C. Lu, M. Yuan, Y. Tian, and H. Zhou, "Acidification of potassium bismuthate for enhanced visible-light photocatalytic degradation ability: an effective strategy for regulating the abilities of adsorption, oxidation, and photocatalysis," *Appl. Surf. Sci.*, vol. 544, p. 148873, 2021.
[27] M. Zulfiqar *et al.*, "Effect of organic solvents on the growth of TiO2 nanotubes: An insight into photocatalytic degradation and adsorption studies," *J. Water Process Eng.*, vol. 37, p. 101491, 2020.
[28] A. A. A. Darwish, M. Rashad, and H. A. AL-Aoh, "Methyl orange adsorption comparison on nanoparticles: Isotherm, kinetics, and thermodynamic studies," *Dye. Pigment.*, vol. 160, pp. 563–571, 2019.
[29] F. Wang, "Adsorption of Anionic Dye on Graphene Nanosheets Doped with Ag Nanoparticles: Kinetics and Thermodynamic Study," *Russ. J. Phys. Chem. A*, vol. 93, no. 7, pp. 1357–1364, 2019.
[30] A. E. Regazzoni, "Adsorption kinetics at solid/aqueous solution interfaces: on the boundaries of the pseudo-second order rate equation," *Colloids Surfaces A Physicochem. Eng. Asp.*, vol. 585, p. 124093, 2020.